

# Rapid, Economical Detection of *Helicobacter pylori* Using Gold Colloidal Nanoparticle Biosensors

Jiaye Jiang, Mathias Charconnet, Ana Galvez Vergara, Shixi Zhang, Yuhan Zhang, Yu Liang, Javier Zubiria, Ane Sorarrain, Jose M. Marimon, Yuan Peng, Lei Zhang,\* and Charles H. Lawrie\*



Cite This: *ACS Omega* 2025, 10, 6559–6566



Read Online

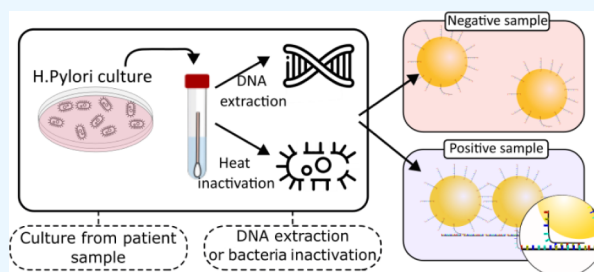
ACCESS |

Metrics & More

Article Recommendations

Supporting Information

**ABSTRACT:** Nucleic acid tests (NAT), the gold standard diagnostic technology, play a crucial role in the prevention of infectious diseases. However, PCR, the current state-of-the-art NAT, is expensive, slow, and requires dedicated infrastructure and facilities. Therefore, there exists an urgent need to create alternative molecular diagnostic technologies. We describe the use of a gold colloidal nanobiosensor detection system that can specifically and sensitively detect the 16S rRNA gene of the worldwide gastric pathogen *Helicobacter pylori*. We demonstrate the systematic identification of oligonucleotide probe sequences according to secondary structure, binding energy, and homology search criteria. We selected three probe sequences that were used to evaluate the detection of a 120 nt synthetic analyte. Detection of this analyte resulted in a visual color change in the solution to a limit of detection (LOD) of 10 nM and by spectrophotometric means to 1 nM. Furthermore, we demonstrated that the system could detect clinical samples of *H. pylori* with a LOD of  $5 \times 10^5$  copies/mL. The system displayed no cross-reactivity with potentially confounding bacterial pathogens. Importantly, we also demonstrated the ability of the detection system to detect clinical samples of *H. pylori* without the requirement of a separate DNA extraction, allowing for a one-step detection system. In summary, we have created a simple-to-use, economical, rapid, sensitive, and specific alternative to PCR that could be useful in resource-limited settings to control the spread of infectious diseases.



## INTRODUCTION

Biosensor-based diagnostics have played a key role in the battle to stop the spread of many infectious diseases including SARS-CoV-2 the causative agent of the recent COVID-19 pandemic.<sup>1</sup> Quantitative reverse transcriptase polymerase chain reaction (qRT-PCR)<sup>2</sup> and to a lesser extent RT loop-mediated isothermal amplification (RT-LAMP)<sup>3</sup> were the most frequently used molecular diagnostic techniques to detect viral RNA, and lateral flow assays (LFA)<sup>4</sup> tests were the most commonly used to detect viral antigens and less commonly antibodies against the SARS-CoV-2 virus. Although PCR and LAMP tests are very sensitive, they are time-consuming, require trained personnel, and are expensive.<sup>5</sup> On the other hand, LFA tests are fast and economical but lack sensitivity under certain circumstances.<sup>6,7</sup> Consequently, there remains great interest in the development of molecular assays that can detect nucleic acids but that are economical and convenient, leading to great interest in nanoparticle detection techniques including gold nanoparticles (AuNPs),<sup>8–10</sup> carbon dots,<sup>11,12</sup> or quantum dots.<sup>13,14</sup> AuNPs in particular are attractive candidates due to their exceptional optical and electronic properties, easy synthesis, and relatively straightforward biofunctionalization chemistries,<sup>15</sup> as their surfaces can be easily modified with various chemical groups, allowing the attachment of oligonucleotides or antibodies.<sup>16,17</sup> This

capability facilitates the detection of target antigens, DNA/RNA, or other molecules, with outputs that can be electrochemical<sup>18</sup> or colorimetric, thanks to plasmonic coupling that arises when two AuNPs are in close proximity.<sup>19–21</sup> As a result of this versatility, AuNPs have been used to develop biosensors to detect a wide variety of organisms including bacteria, viruses, and fungi.<sup>10,22–24</sup> In particular, AuNPs functionalized with oligonucleotides have been used for the fast colorimetric detection of *Chlamydia trachomatis* and *Neisseria gonorrhoeae*,<sup>25</sup> hepatitis C virus (HCV),<sup>26</sup> and SARS-CoV-2 virus.<sup>23</sup> However, to date, the choice of oligonucleotide probes that are effective in detecting pathogens for this technology has been an empirical exercise, resulting in the generation and testing of many oligos in order to optimize detection. In this article, we propose the use of ViennaRNA 2.5<sup>27,28</sup> nucleic acid-folding package to calculate DNA/RNA interactions in order to more efficiently select oligos for the development of a rapid

**Received:** August 5, 2024  
**Revised:** January 14, 2025  
**Accepted:** January 15, 2025  
**Published:** February 11, 2025



molecular assay to detect the *Helicobacter pylori* (*H. pylori*) pathogen.

Infection by *H. pylori*, a Gram-negative, spiral-shaped bacterium, occurs in up to 50% of the global population, and although generally asymptomatic, it is a frequent cause of stomach ulcers and even cancer.<sup>29,30</sup> However, the rate of *H. pylori* infection has decreased to less than 40% due to better food preparation hygiene in most countries,<sup>31</sup> in some developing countries rates remain stubbornly over 70%.<sup>30,32</sup>

In addition to the use of qPCR and endoscopic biopsy, the most frequently used diagnostic testing technique for *H. pylori* is the urea breath test (UBT), which requires prior oral administration of labeled urea (<sup>13</sup>C/<sup>14</sup>C). This method is, however, uncomfortable for the patient and requires the use of specialized instrumentation. Fecal antigen LFAs are also widely used, especially for pediatric testing; however, many adults are uncomfortable with sampling<sup>33</sup> and commonly used proton-pump inhibitors (PPIs)<sup>34</sup> and antibiotics can interfere with results.<sup>35</sup> More recently, detection techniques based on electrochemistry, in particular using self-assembled gold NPs on graphene oxide or carbon nanotubes, have shown the detection of *H. pylori* DNA or proteins with great sensitivity.<sup>36</sup>

As we had previously developed a method for the direct detection of SARS-CoV-2 from saliva and nasopharyngeal samples using AuNPs,<sup>23</sup> we extended this work to *H. pylori* based on the detection of the 16S rRNA. We developed a novel *in silico* selection criterion based upon the ViennaRNA 2.5 RNA folding algorithm and tested our system on clinical samples of *H. pylori* and other potentially interfering bacteria.

## EXPERIMENTAL SECTION

**Materials.** NanoXact 60 nm nanospheres in 0.05 mg/mL citrate buffer (1.5 OD) were purchased from NanoComposix (San Diego, USA) with a diameter of  $61 \pm 6$  nm (characterized by transmission electron microscopy (JEOL 1010), a surface charge of  $-40$  mV, and a plasmon resonance wavelength of 535 nm (characterized by dynamic light scattering (Malvern Nano ZS) and UV-vis spectrophotometer (Persee)). S'-SH conjugated oligonucleotides were synthesized by Generay Biotech (Shanghai, China). Sodium dodecyl sulfate (SDS), 1 M phosphate buffer pH 7.4, and Triton X-100 were purchased from Sigma-Aldrich (St. Louis, USA), Tris-HCl pH 8.0 and EDTA from Beyotime Biotechnology (Shanghai, China), and proteinase K from GeneOn (Ludwigshafen, Germany). Dynamic light scattering measurements were taken using Optronix Technology (Shanghai, China), and UV-vis measurements were performed using an Agilent BioTek Synergy 2 plate reader (Santa Clara, CA) and Persee Analytics UV-vis spectrophotometer (Auburn, CA).

**Oligonucleotide Design.** Sequences of the 16S rRNA gene were recovered from GenBank (accession numbers can be found in Figure S1); only complete sequences were considered. Oligonucleotides were selected by calculating secondary structure, self-binding energy, and binding energy to target using ViennaRNA 2.5 software,<sup>27,28</sup> considering a temperature of 25 °C and [NaCl] = 1 M. Secondary structure minimum free energy was calculated using the RNAfold function provided in ViennaRNA 2.5, while binding energy between oligonucleotides and the 16S rRNA gene was calculated using RNAcofold also provided in ViennaRNA 2.5. Oligonucleotides were then selected on the basis of fulfilling the following criteria:

Secondary Structure energy = 0 kcal/mol (no secondary structure): oligonucleotides presenting secondary structures were not selected since this can result in lower hybridization of the oligonucleotide to the complementary target<sup>37,38</sup> but also reduce the stability of the AuNPs due to lower grafting density and lower layer thickness, which promote aggregation between nanoparticles.<sup>39,40</sup>

Self-binding energy <9 kcal/mol: Dimerization energy of the oligonucleotides to itself and to other oligonucleotides used in the assay were minimized. Dimerization energy should be lower than 9 kcal/mol in absolute value.

Binding energy >20 kcal/mol: Binding energy was maximized in order to get optimal binding of the nanoparticles to the target nucleic acid.

The specificity of the selected oligonucleotides was checked using the BLAST algorithm,<sup>41</sup> and the binding energies of the oligonucleotide to the 16S rRNA gene of different bacteria were calculated using the RNAcofold function within the ViennaRNA 2.5 package.

**AuNPs' Functionalization.** AuNPs were functionalized using thiolated oligonucleotides and a previously reported salt-aging method.<sup>42</sup> In brief, AuNPs were resuspended in 0.005% sodium dodecyl sulfate (SDS) and 0.05 M phosphate buffer (PBS), pH 7.8, before adding oligonucleotides to attain an oligonucleotide concentration of 2 μM. Subsequently, the NaCl concentration was gradually increased until reaching 0.1 M NaCl in order to increase the density of oligonucleotides bound to the AuNPs' surface.

**Limit of Detection (LOD) Assay.** A 120 nt DNA sequence covering 540–660 nt of the 16S rRNA gene was used as a positive control analyte (Generay Biotech). For LOD determination, the positive control was spiked into lysis buffer (0.11% SDS, 0.11% Triton X-100, 0.58 mg/mL Proteinase K, TE buffer ×1) in a series of half-log<sub>10</sub> dilutions (*i.e.*, 100 nM, 33 nM, 10 nM, 3.3 nM, 1 nM, and 0 nM (negative)). For each test, 8.5 μL of functionalized nanoparticles was added to 47.5 μL of lysis buffer (0.11% SDS, 0.11% Triton X-100, 0.58 mg/mL Proteinase K, TE buffer ×1), and a desired amount of 5 M NaCl was added subsequently. All reactions were carried out at room temperature.

**Cultures and Extraction of *H. pylori*.** Patient gastro-duodenal biopsies were cultured immediately on arrival to the laboratory on marketed selective plates (Pylori Agar; bioMérieux, Marcy-l'Étoile, France). Plates were incubated under microaerophilic conditions (2% H<sub>2</sub>, 5% O<sub>2</sub>, 7% CO<sub>2</sub>, and 86% N<sub>2</sub>) at 37 °C with 80% humidity for at least 7 days. Colonies were confirmed as *H. pylori* using matrix-assisted laser desorption ionization-time-of-flight mass spectrometry (MALDI-TOF-MS, MALDI Biotyper, Bruker Daltonics).

DNA extraction was carried out on heat-inactivated samples (90 °C for 10 min) using the Qiagen DNA Blood Mini Kit according to the manufacturer's instructions (Qiagen, Hilden, Germany).

## RESULTS AND DISCUSSION

**Oligonucleotide Design.** The detection of *H. pylori* in this study was based on the color change of AuNPs in solution upon binding to the target analyte. When dispersed, AuNPs display a red color in solution but appear bluish/transparent upon binding to multiple DNA/RNA target analytes, resulting in agglomeration of the nanoparticles due to plasmonic

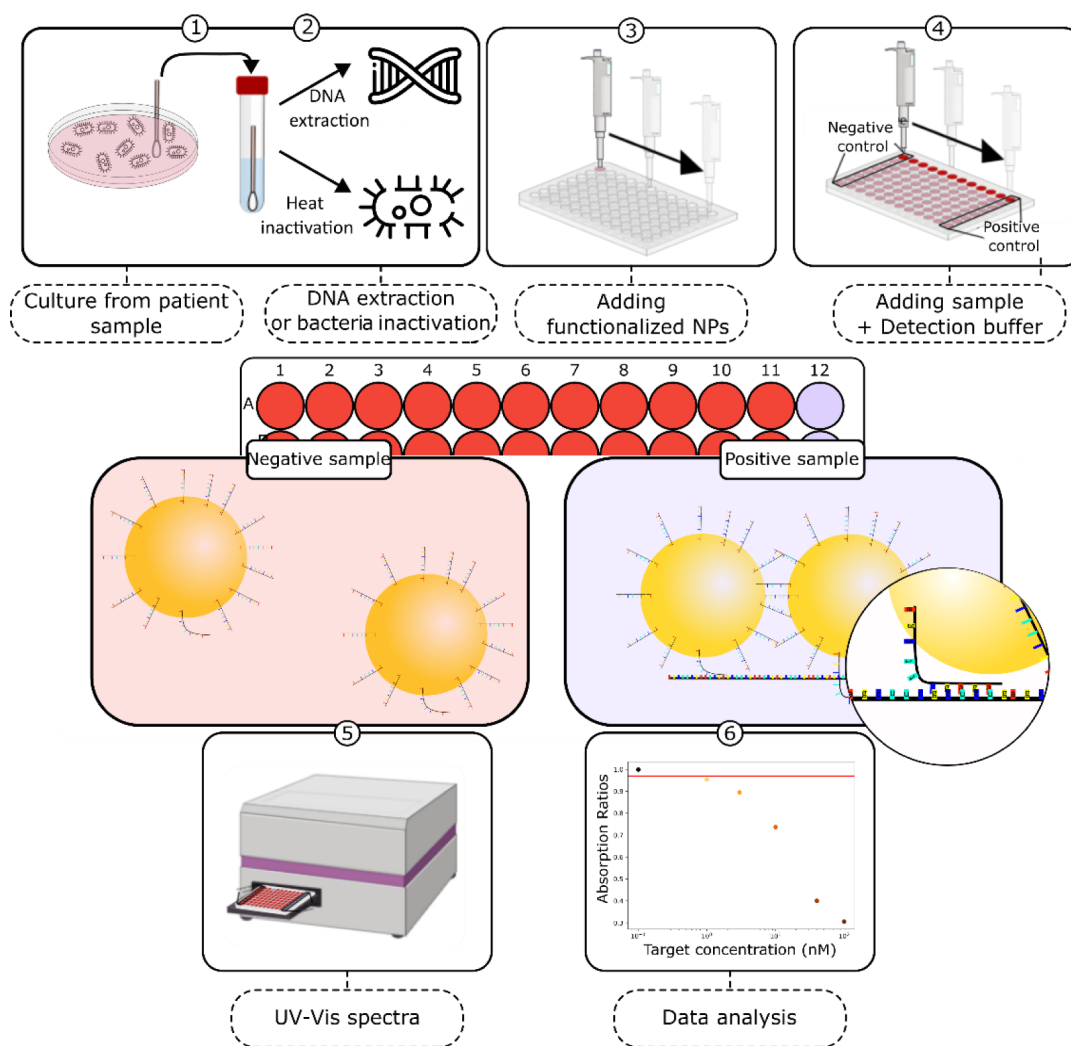


**Figure 1.** Scheme for the validation of the *H. pylori* assay.

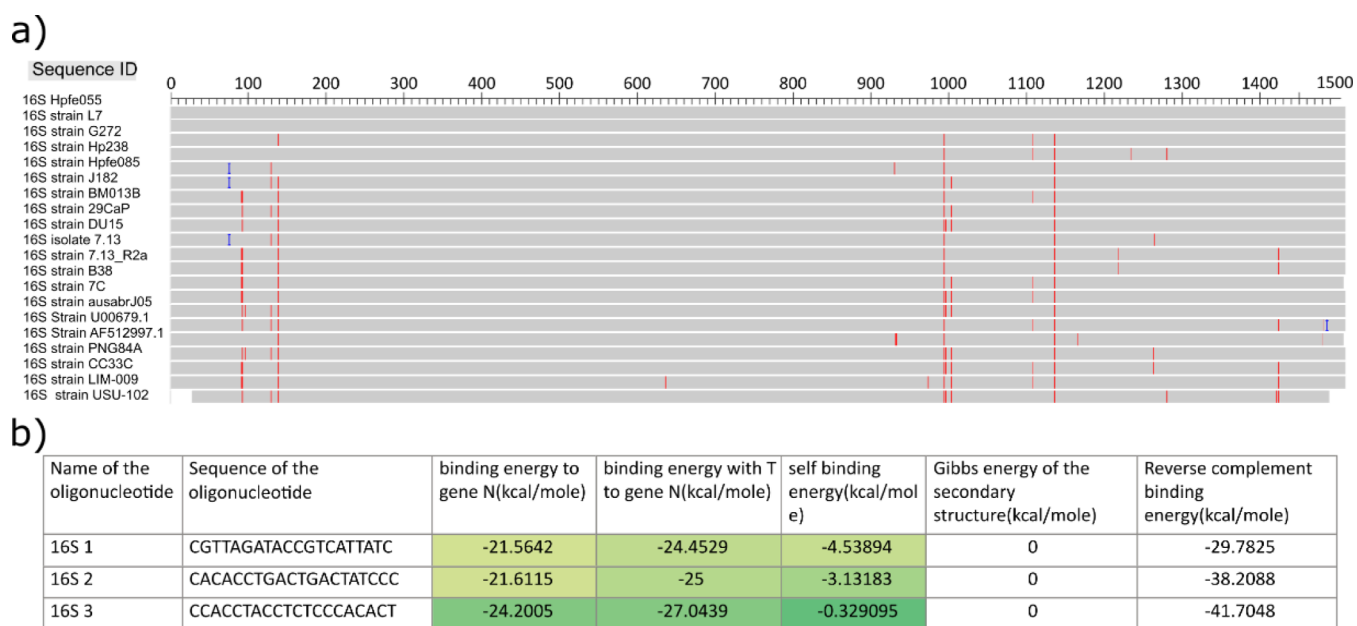


**Figure 2.** Oligonucleotides selection. (a) Alignment of different *H. pylori* strains on their 16S rRNA gene. (b) Table containing the different selected oligonucleotides with their calculated binding energy with and without T10 spacer, self-binding energy, and secondary structure energy.

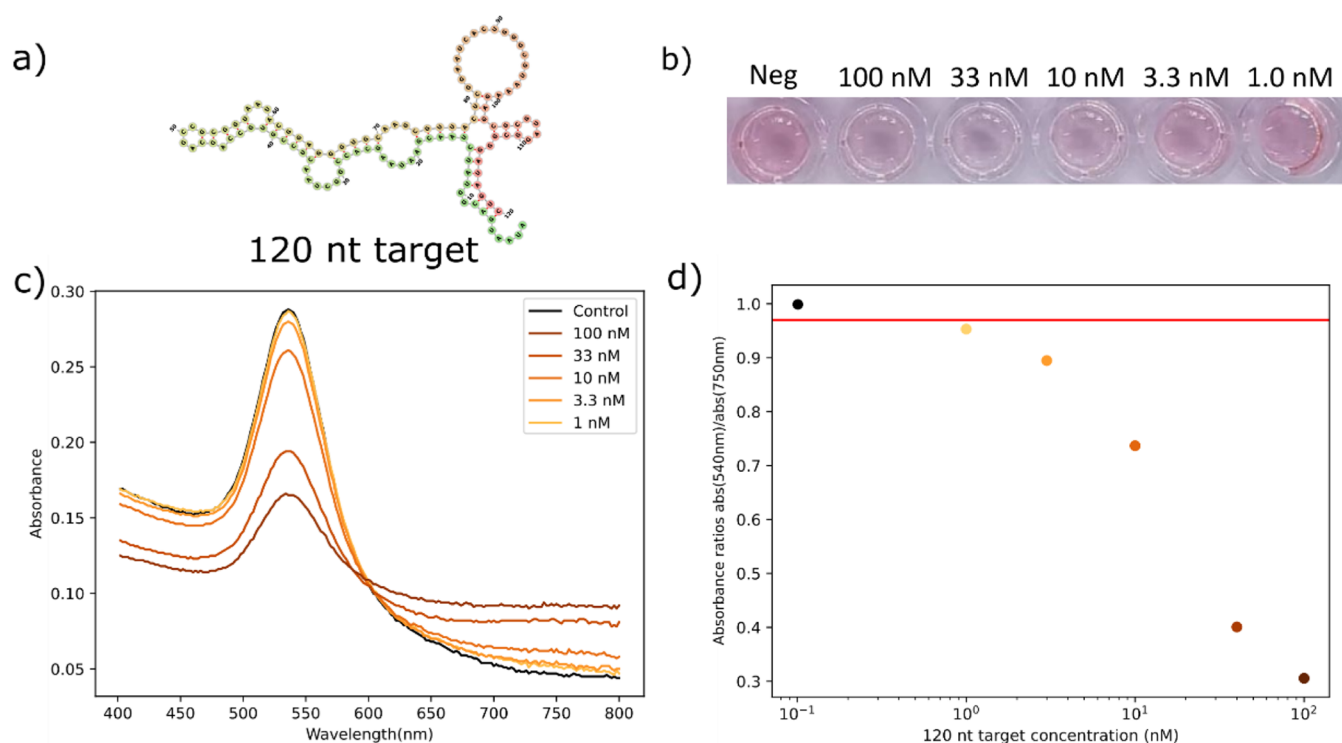


**Figure 3.** 120 nt short target detection. (a) Secondary structure of the 120 nt short target. (b) Image, (c) UV–vis spectra, and (d) absorbance ratio (540/750 nm) of the limit of detection assay using the 120 nt short target mimicking targeted region of the 16S rRNA gene.

coupling<sup>43</sup> (as depicted in Figure 1). This color change can be monitored either by UV–vis spectroscopy or by the naked eye.

The 16S rRNA gene was selected in this study as the target for the detection of *H. pylori* due to high levels of homology between different strains of *H. pylori* (Figure 2a) and the presence of hypervariable regions (HVRs), which enable to distinguish between *H. pylori* and other common bacteria such as *Campylobacter* spp.<sup>44</sup> As can be seen from Figure 2a, the sequence of the 16S rRNA gene is highly conserved between different *H. pylori* strains with only a few nucleotide variations observed at positions 92, 129, 138, 991, 1000, 1105, and 1133 of the gene. Consequently, we selected all possible 20 nt combinations that covered the HVR and surrounding regions and calculated their binding energy, secondary structure, and self-binding energy (Figure S3).

Based on this information, we selected three oligonucleotides (16S#1, 16S#2, and 16S#3; Figure 2b) and calculated the binding energy to the 16S rRNA gene with and without a T(10) spacer sequence. We observed that oligonucleotides with a T10 spacer exhibited higher binding energy toward the target due to higher base pairing. As it is known that the presence of a T10 spacer increases the binding efficiency to AuNPs as well as increasing the efficiency of probe binding by decreasing spatial hindrance, we used these oligos for subsequent experiments.

In order to check the specificity of the selected oligonucleotides, we used the BLAST alignment algorithm as well as calculating the binding energy to closely related bacteria (*Campylobacter jejuni*, *Enterobacter cloacae* etc.) (Figures S4–S6). There were no major homology matches between the selected oligonucleotides and other microorganisms within the NCBI database. We additionally calculated the binding energy between the selected oligonucleotides and the 16S rRNA gene

of other bacteria and observed much lower binding energies than those with *H. pylori* (Figure S7).

**AuNPs' Functionalization.** Oligonucleotides with a thiol moiety on their 5' end were attached to the AuNPs' surface using the salt-aging method as described above. After functionalization, AuNPs underwent a change in diameter from  $67 \pm 1$  nm to  $90.5 \pm 1$  nm as measured by DLS (Figure S8). Additionally, their surface zeta potential charge changed from  $-47.4 \pm 5.5$  mV to  $-33.0 \pm 5.5$  mV (Figure S8). We also carried out UV–vis spectra of the AuNPs (Figure S8) and observed a shift of the plasmon resonance from 535 to 538 nm due to the change of refractive index in the close vicinity of the AuNPs after the binding of the oligonucleotides. Furthermore, the cost of the functionalized NPs including the functionalization reagents as well as detection reagents was 0.66 euros, constituting a price that could compete with antigen tests (see details of prices in Figure S9).

**Detection of 120 nt Analyte.** Functionalized AuNPs were then tested for the detection of a synthetic target analyte (120 nt DNA of the *H. pylori* 16S gene, including target sequences of three oligos) (Figure 3a). To determine the limit of detection (LOD) of the assay, the analyte was serially diluted to different concentrations and spiked into lysis buffer. We tested lysis buffer without analyte (negative control) and observed a shift of the plasmon resonance wavelength from 538 to 540 nm due to a change in the refractive index of the solution. As can be seen from Figure 3c, the plasmon resonance wavelength decreases from 540 nm in the presence of the analyte due to plasmonic coupling between the AuNPs caused by the hybridization of the oligonucleotide probes and their complementary target. This agglomeration results in a decrease in the 540/750 nm absorbance ratio (Figure 3d). This optical change can also be observed by the naked eye, resulting in a color change from pink to blue/transparent

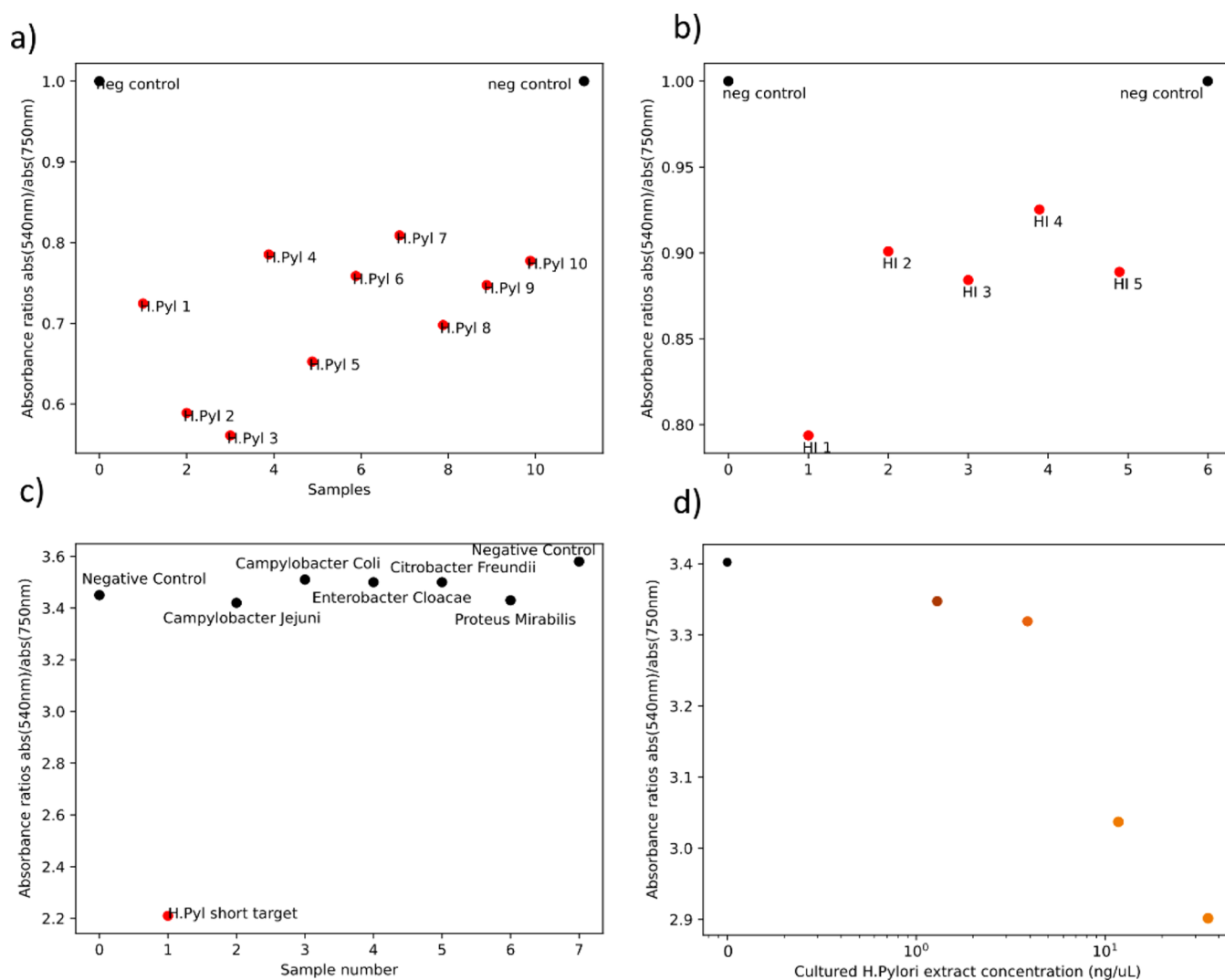


**Figure 4.** Detection of cultured samples from different patients infected with different bacteria, (a) absorbance ratio of assays containing extracts from cultures of *H. pylori* obtained from different patients, (b) absorbance ratio of assays containing heat inactivated cultures of *H. pylori* obtained from different patients, (c) absorbance ratio of assays containing different concentrations of cultured extracts from different bacteria, and (d) absorbance ratio of assays containing different concentrations of cultured *H. pylori* extract.

(Figure 3b). The LOD of observation by the naked eye was 10 nM, whereas by spectrophotometric means it was 1 nM (Figure 3d).

**Detection of Clinical Samples.** Although the 120 nt analyte is useful to characterize the ability of AuNPs to detect the target of interest, as the 16S rRNA gene is ~1600 nt in length, it might be more challenging to detect due to the crowding effects of longer nucleic acids. We therefore tested our system with either extracted DNA or whole bacteria from cultured *H. pylori* taken from patient's samples. As can be seen from Figure 4a, we were able to detect all 10 (100%) of the tested DNA extracts from patient-cultured *H. pylori* bacteria, as depicted by the lower 540/750 nm absorbance ratio. In order to increase the potential utility of the test, we also tested whole heat-inactivated *H. pylori* bacteria from patients. Again, we note that we can detect all 10 samples without the need for a separate DNA extraction step (Figure 4b).

In order to further characterize the assay, we next carried out cross-reactivity tests with DNA extracts from cultures of the following potentially confounding bacteria: *Proteus mirabilis*, *Enterobacter cloacae*, *Campylobacter jejuni*, *Campylobacter coli*,

and *Citrobacter freundii*. As can be seen from Figure 4c, only *H. pylori* DNA was detected. A lack of cross-reactivity with *C. jejuni* is potentially useful as not only is infection by this bacterium often mistaken for *H. pylori* infection, but it also displays a high degree of homology within the 16S rRNA gene (~87%).

In order to compare the LOD of clinical *H. pylori* samples, we serially diluted DNA obtained from cultured *H. pylori*. As can be seen, the LOD was determined to be 1 ng/ $\mu$ L, which corresponds to around  $5 \times 10^5$  copies/mL (Figure 4d).

## CONCLUSIONS

In this article, we chose 16S rRNA due to its conservation among different *H. pylori* strains and the presence of hypervariable regions that distinguish it from other common bacteria. The selected oligonucleotides were tested for their binding energy, secondary structure, and specificity using ViennaRNA and BLAST alignment software for a specificity check. The selected oligonucleotides were then successfully attached to AuNPs by attaching thiol moieties on their 5' end and using a salt-aging method.

Our assay demonstrated the effective detection of a 120 nt target covering part of the 16S rRNA gene of *H. pylori*. Detection of this analyte resulted in a clear color change observable by the naked eye as well as by UV–vis spectroscopy. The assay successfully detected *H. pylori* in both extracted DNA/RNA from cultured samples and heat-inactivated cultured samples, with no cross-reactivity observed with closely related bacteria such as *Campylobacter jejuni*. 10/10 (100%) of the cultured samples from different patients' gastroduodenal biopsy were detected, highlighting the robustness of our assay. The limit of detection was determined to be 1 ng/ $\mu$ L of *H. pylori* nucleic acids, corresponding to approximately  $5 \times 10^5$  copies/mL of the 16S rRNA from *H. pylori*.

In conclusion, our study presents a robust and specific assay for detecting *H. pylori* using gold nanoparticles functionalized with *in silico* designed oligonucleotides. This approach not only provides a reliable diagnostic tool for *H. pylori* but also offers a versatile platform for developing similar assays for other microorganisms with a cost under 1 euro for a single test. Indeed, the *in silico* workflow for oligonucleotide selection can be easily adapted for detecting a broad range of viruses, bacteria, and fungi.

## ■ ASSOCIATED CONTENT

### SI Supporting Information

The Supporting Information is available free of charge at <https://pubs.acs.org/doi/10.1021/acsomega.4c07170>.

16S rRNA accession numbers for different strains of *Helicobacter pylori*; hypervariable regions of the 16S rRNA; the oligonucleotides and target sequences used in the experiments; BLAST results of oligonucleotide 16S 1–3; binding energies of the oligonucleotides; UV–vis spectra, Z-sizer, and Z-potential measurements; price detail for a single test (PDF)

## ■ AUTHOR INFORMATION

### Corresponding Authors

**Lei Zhang** – Sino-Swiss Institute of Advanced Technology (SSIAT), Shanghai University, Shanghai 201800, China; School of Microelectronics, Shanghai University, Shanghai 201899, China; Email: [zhangleich@shu.edu.cn](mailto:zhangleich@shu.edu.cn)

**Charles H. Lawrie** – Sino-Swiss Institute of Advanced Technology (SSIAT), Shanghai University, Shanghai 201800, China; Molecular Oncology Group, Biogipuzkoa Health Research Institute, Donostia-San Sebastian, Spain 20014; IKERBASQUE, Basque Foundation for Science, Bilbao 48009, Spain; Radcliffe Department of Medicine, University of Oxford, Oxford OX1 2JD, U. K.; [orcid.org/0000-0002-8882-1131](https://orcid.org/0000-0002-8882-1131); Email: [charles.lawrie@biogipuzkoa.eus](mailto:charles.lawrie@biogipuzkoa.eus)

### Authors

**Jiaye Jiang** – College of Sciences, Shanghai University, Shanghai 201800, China; Sino-Swiss Institute of Advanced Technology (SSIAT), Shanghai University, Shanghai 201800, China

**Mathias Charconnet** – Sino-Swiss Institute of Advanced Technology (SSIAT), Shanghai University, Shanghai 201800, China

**Ana Galvez Vergara** – Sino-Swiss Institute of Advanced Technology (SSIAT), Shanghai University, Shanghai 201800, China

**Shixi Zhang** – Sino-Swiss Institute of Advanced Technology (SSIAT), Shanghai University, Shanghai 201800, China

**Yuhan Zhang** – Sino-Swiss Institute of Advanced Technology (SSIAT), Shanghai University, Shanghai 201800, China

**Yu Liang** – Shanghai Institute of Biotech, Shanghai 200444, China

**Javier Zubiria** – Sino-Swiss Institute of Advanced Technology (SSIAT), Shanghai University, Shanghai 201800, China

**Ane Sorarrain** – Respiratory Infection and Antimicrobial Resistance Group, Biogipuzkoa Health Research Institute, Donostia-San Sebastian 20014, Spain; Microbiology Department, Osakidetza Basque Health Service, Donostialdea Integrated Health Organization, Donostia-San Sebastian 20014, Spain

**Jose M. Marimon** – Respiratory Infection and Antimicrobial Resistance Group, Biogipuzkoa Health Research Institute, Donostia-San Sebastian 20014, Spain; Microbiology Department, Osakidetza Basque Health Service, Donostialdea Integrated Health Organization, Donostia-San Sebastian 20014, Spain

**Yuan Peng** – Sino-Swiss Institute of Advanced Technology (SSIAT), Shanghai University, Shanghai 201800, China

Complete contact information is available at:

<https://pubs.acs.org/10.1021/acsomega.4c07170>

### Author Contributions

The manuscript was written through the contributions of all authors. All authors have given approval to the final version of the manuscript. J.J.: conceptualization, data curation, and writing the original draft. M.C.: conceptualization, data curation, writing, review, and editing. A.G.V.: conceptualization, data curation, writing, review, and editing. S.Z.: data curation and formal analysis. Y.Z.: data curation and formal analysis. Y.L.: data curation, writing, review, and editing. J.Z.: conceptualization, data curation. A.S.: data curation and formal analysis. J.M.M.: data curation and formal analysis. Y.P.: data curation and formal analysis. L.Z.: conceptualization, supervision, funding acquisition, resources, review, and editing. C.H.L.: conceptualization, supervision, funding acquisition, resources, review, and editing.

### Notes

The authors declare no competing financial interest.

## ■ ACKNOWLEDGMENTS

The authors are grateful to Shanghai University for their support.

## ■ REFERENCES

- (1) Goggolidou, P.; Hodges-Mameletzis, I.; Purewal, S.; Karakoula, A.; Warr, T. Self-Testing as an Invaluable Tool in Fighting the COVID-19 Pandemic. *J. Prim Care Community Health* **2021**, *12*, 21501327211047782.
- (2) Smyrlaki, I.; Ekman, M.; Lentini, A.; Rufino de Sousa, N.; Papanicolaou, N.; Vondracek, M.; Aarum, J.; Safari, H.; Muradrasoli, S.; Rothfuchs, A. G.; Albert, J.; Högberg, B.; Reinius, B. Massive and Rapid COVID-19 Testing Is Feasible by Extraction-Free SARS-CoV-2 RT-PCR. *Nat. Commun.* **2020**, *11* (1), 1–12.
- (3) Lim, B.; Ratcliff, J.; Nawrot, D. A.; Yu, Y.; Sanghani, H. R.; Hsu, C.-C.; Peto, L.; Evans, S.; Hodgson, S. H.; Skeva, A.; et al. Clinical

Validation of Optimised RT-LAMP for the Diagnosis of SARS-CoV-2 Infection. *Sci. Rep.* **2021**, *11* (1), 16193.

(4) Hsieh, W.-Y.; Lin, C.-H.; Lin, T.-C.; Lin, C.-H.; Chang, H.-F.; Tsai, C.-H.; Wu, H.-T.; Lin, C.-S. Development and Efficacy of Lateral Flow Point-of-Care Testing Devices for Rapid and Mass COVID-19 Diagnosis by the Detections of SARS-CoV-2 Antigen and Anti-SARS-CoV-2 Antibodies. *Diagnostics* **2021**, *11* (10), 1760.

(5) Song, X.; Coulter, F. J.; Yang, M.; Smith, J. L.; Tafesse, F. G.; Messer, W. B.; Reif, J. H. A Lyophilized Colorimetric RT-LAMP Test Kit for Rapid, Low-Cost, at-Home Molecular Testing of SARS-CoV-2 and Other Pathogens. *Sci. Rep.* **2022**, *12* (1), 7043.

(6) Peto, T.; Affron, D.; Afrough, B.; Agasu, A.; Ainsworth, M.; Allanson, A.; Allen, K.; Allen, C.; Archer, L.; Ashbridge, N.; et al. COVID-19: Rapid Antigen Detection for SARS-CoV-2 by Lateral Flow Assay: A National Systematic Evaluation of Sensitivity and Specificity for Mass-Testing. *EClinicalMedicine* **2021**, *36*, 100924.

(7) Mistry, D. A.; Wang, J. Y.; Moeser, M.-E.; Starkey, T.; Lee, L. Y. W. A Systematic Review of the Sensitivity and Specificity of Lateral Flow Devices in the Detection of SARS-CoV-2. *BMC Infect. Dis.* **2021**, *21* (1), 828.

(8) Halo, T. L.; McMahon, K. M.; Angeloni, N. L.; Xu, Y.; Wang, W.; Chinen, A. B.; Malin, D.; Strelakova, E.; Cryns, V. L.; Cheng, C.; Mirkin, C. A.; Thaxton, C. S. NanoFlares for the Detection, Isolation, and Culture of Live Tumor Cells from Human Blood. *Proc. Natl. Acad. Sci. U. S. A.* **2014**, *111* (48), 17104–17109.

(9) Son, J. H.; Cho, B.; Hong, S.; Lee, S. H.; Hoxha, O.; Haack, A. J.; Lee, L. P. Ultrafast Photonic PCR. *Light: Sci. Appl.* **2015**, *4* (7), No. e280–e280.

(10) Moitra, P.; Alafeef, M.; Dighe, K.; Frieman, M. B.; Pan, D. Selective Naked-Eye Detection of SARS-CoV-2 Mediated by N Gene Targeted Antisense Oligonucleotide Capped Plasmonic Nanoparticles. *ACS Nano* **2020**, *14* (6), 7617–7627.

(11) Belza, J.; Oplová, A.; Poláková, K.; et al. Carbon Dots for Virus Detection and Therapy. *Microchim. Acta* **2021**, *188* (12), 430.

(12) Sheffield, Z.; Alafeef, M.; Moitra, P.; Ray, P.; Pan, D. N-Gene-Complementary Antisense-Oligonucleotide Directed Molecular Aggregation of Dual-Colour Carbon Dots, Leading to Efficient Fluorometric Sensing of SARS-COV-2 RNA. *Nanoscale* **2022**, *14* (13), 5112–5120.

(13) Chiang, W.; Stout, A.; Yanchik-Slade, F.; Li, H.; Terrando, N.; Nilsson, B. L.; Gelbard, H. A.; Krauss, T. D. Quantum Dot Biomimetic for SARS-CoV-2 to Interrogate Blood–Brain Barrier Damage Relevant to NeuroCOVID Brain Inflammation. *ACS Appl. Nano Mater.* **2023**, *6* (16), 15094–15107.

(14) Wang, X.; Shao, S.; Ye, H.; Li, S.; Gu, B.; Tang, B. Development of a Quantum Dot-Based Lateral Flow Immunoassay Strip for Rapid and Sensitive Detection of SARS-CoV-2 Neutralizing Antibodies. *Sci. Rep.* **2023**, *13* (1), 22253.

(15) Ma, X.; Li, X.; Luo, G.; Jiao, J. DNA-Functionalized Gold Nanoparticles: Modification, Characterization, and Biomedical Applications. *Front. Chem.* **2022**, *10*, 1095488.

(16) Jazayeri, M. H.; Amani, H.; Pourfatollah, A. A.; Pazoki-Toroudi, H.; Sedighimoghaddam, B. Various Methods of Gold Nanoparticles (GNPs) Conjugation to Antibodies. *Sens Biosensing Res.* **2016**, *9*, 17–22.

(17) Liu, B.; Wu, P.; Huang, Z.; Ma, L.; Liu, J. Bromide as a Robust Backfiller on Gold for Precise Control of DNA Conformation and High Stability of Spherical Nucleic Acids. *J. Am. Chem. Soc.* **2018**, *140* (13), 4499–4502.

(18) Aydinlik, S.; Ozkan-Ariksoyals, D.; Kara, P.; Sayiner, A. A.; Ozsoz, M. A Nucleic Acid-Based Electrochemical Biosensor for the Detection of Influenza B Virus from PCR Samples Using Gold Nanoparticle-Adsorbed Disposable Graphite Electrode and Meldola's Blue as an Intercalator. *Anal. Methods* **2011**, *3* (7), 1607.

(19) Enoch, S.; Bonod, N. Plasmonics In *From Basics to Advanced Topics*; Springer: Berlin, Heidelberg, 2012; Vol. 167, .

(20) Yoon, J. H.; Selbach, F.; Langolf, L.; Schlücker, S. Ideal Dimers of Gold Nanospheres for Precision Plasmonics: Synthesis and

Characterization at the Single-Particle Level for Identification of Higher Order Modes. *Small* **2018**, *14* (4), 1–5.

(21) Slaughter, L. S.; Willingham, B. A.; Chang, W. S.; Chester, M. H.; Ogden, N.; Link, S. Toward Plasmonic Polymers. *Nano Lett.* **2012**, *12* (8), 3967–3972.

(22) Lee, J. I.; Jang, S. C.; Chung, J.; Choi, W.-K.; Hong, C.; Ahn, G. R.; Kim, S. H.; Lee, B. Y.; Chung, W.-J. Colorimetric Allergenic Fungal Spore Detection Using Peptide-Modified Gold Nanoparticles. *Sens. Actuators, B* **2021**, *327*, 128894.

(23) Armesto, M.; Charconnet, M.; Marimón, J. M.; Fernández Regueiro, C. L.; Jia, J.; Yan, T.; Sorarrain, A.; Grzelczak, M.; Sanromán, M.; Vicente, M.; Klempa, B.; Zubiria, J.; Peng, Y.; Zhang, L.; Zhang, J.; Lawrie, C. H. Validation of Rapid and Economic Colorimetric Nanoparticle Assay for SARS-CoV-2 RNA Detection in Saliva and Nasopharyngeal Swabs. *Biosensors* **2023**, *13* (2), 275.

(24) Schmitz, F. R. W.; Cesca, K.; Valério, A.; de Oliveira, D.; Hotza, N. D. Colorimetric Detection of Pseudomonas Aeruginosa by Aptamer-Functionalized Gold Nanoparticles. *Appl. Microbiol. Biotechnol.* **2023**, *107* (1), 71–80.

(25) Dighe, K.; Moitra, P.; Gunaseelan, N.; Alafeef, M.; Jensen, T.; Rafferty, C.; Pan, D. Highly-Specific Single-Stranded Oligonucleotides and Functional Nanoprobe for Clinical Determination of Chlamydia Trachomatis and Neisseria Gonorrhoeae Infections. *Adv. Sci.* **2023**, *10* (36), 2304009.

(26) Mohammed, A. S.; Balapure, A.; Khaja, M. N.; Ganesan, R.; Dutta, J. R. Naked-Eye Colorimetric Detection of HCV RNA Mediated by a 5'UTR-Targeted Antisense Oligonucleotide and Plasmonic Gold Nanoparticles. *Analyst* **2021**, *146* (5), 1569–1578.

(27) Lorenz, R.; Bernhart, S. H.; Höner Zu Siederdisen, C.; Tafer, H.; Flamm, C.; Stadler, P. F.; Hofacker, I. L. ViennaRNA Package 2.0. *Algorithms Mol. Biol.* **2011**, *6* (1), 26.

(28) Yao, H.-T.; Lorenz, R.; Hofacker, I. L.; Stadler, P. F. Mono-Valent Salt Corrections for RNA Secondary Structures in the ViennaRNA Package. *Algorithms Mol. Biol.* **2023**, *18* (1), 8.

(29) Yu, M.; Ma, J.; Song, X.-X.; Shao, Q.-Q.; Yu, X.-C.; Khan, M. N.; Qi, Y.-B.; Hu, R.-B.; Wei, P.-R.; Xiao, W.; Jia, B.-L.; Cheng, Y.-B.; Kong, L.-F.; Chen, C.-L.; Ding, S.-Z. Gastric Mucosal Precancerous Lesions in *Helicobacter Pylori* -Infected Pediatric Patients in Central China: A Single-Center, Retrospective Investigation. *World J. Gastroenterol.* **2022**, *28* (28), 3682–3694.

(30) Wang, H.; Zhao, M.; Shi, F.; Zheng, S.; Xiong, L.; Zheng, L. A Review of Signal Pathway Induced by Virulent Protein CagA of *Helicobacter Pylori*. *Front. Cell. Infect. Microbiol.* **2023**, *13*, 1062803.

(31) Öztekin, M.; Yılmaz, B.; Ağagündüz, D.; Capasso, R. Overview of *Helicobacter Pylori* Infection: Clinical Features, Treatment, and Nutritional Aspects. *Diseases* **2021**, *9* (4), 66.

(32) Hooi, J. K. Y.; Lai, W. Y.; Ng, W. K.; Suen, M. M. Y.; Underwood, F. E.; Tanyingoh, D.; Malfertheiner, P.; Graham, D. Y.; Wong, V. W. S.; Wu, J. C. Y.; Chan, F. K. L.; Sung, J. J. Y.; Kaplan, G. G.; Ng, S. C. Global Prevalence of *Helicobacter Pylori* Infection: Systematic Review and Meta-Analysis. *Gastroenterology* **2017**, *153* (2), 420–429.

(33) Yang, H. R.; Seo, J. K. *Helicobacter Pylori* Stool Antigen (HpSA) Tests in Children Before and After Eradication Therapy: Comparison of Rapid Immunochromatographic Assay and HpSA ELISA. *Dig. Dis. Sci.* **2008**, *53* (8), 2053–2058.

(34) Korkmaz, H.; Kesli, R.; Karabagli, P.; Terzi, Y. Comparison of the Diagnostic Accuracy of Five Different Stool Antigen Tests for the Diagnosis of *Helicobacter Pylori* Infection. *Helicobacter* **2013**, *18* (5), 384–391.

(35) Celiberto, F.; Losurdo, G.; Pricci, M.; Girardi, B.; Marotti, A.; Di Leo, A.; Ierardi, E. The State of the Art of Molecular Fecal Investigations for *Helicobacter Pylori* (H. Pylori) Antibiotic Resistances. *Int. J. Mol. Sci.* **2023**, *24* (5), 4361.

(36) Hajhosseini, S.; Nasirizadeh, N.; Hejazi, M. S.; Yaghmaei, P. A Sensitive DNA Biosensor Fabricated from Gold Nanoparticles and Graphene Oxide on a Glassy Carbon Electrode. *Mater. Sci. Eng.* **2016**, *61*, 506–515.

- (37) Mann, T.; Humbert, R.; Dorschner, M.; Stamatoyannopoulos, J.; Noble, W. S. A Thermodynamic Approach to PCR Primer Design. *Nucleic Acids Res.* **2009**, *37* (13), No. e95–e95.
- (38) Rychlik, W. Selection of Primers for Polymerase Chain Reaction. In *PCR Protocols*; Humana Press: NJ, pp. 31–40. .
- (39) Peng, B.; Liu, Z.; Jiang, Y. Aggregation of DNA-Grafted Nanoparticles in Water: The Critical Role of Sequence-Dependent Conformation of DNA Coating. *J. Phys. Chem. B* **2022**, *126* (4), 847–857.
- (40) Parak, W. J.; Pellegrino, T.; Micheel, C. M.; Gerion, D.; Williams, S. C.; Alivisatos, A. P. Conformation of Oligonucleotides Attached to Gold Nanocrystals Probed by Gel Electrophoresis. *Nano Lett.* **2003**, *3* (1), 33–36.
- (41) McGinnis, S.; Madden, T. L. BLAST: At the Core of a Powerful and Diverse Set of Sequence Analysis Tools. *Nucleic Acids Res.* **2004**, *32* (Web Server), W20–W25.
- (42) Hurst, S. J.; Lytton-Jean, A. K. R.; Mirkin, C. A. Maximizing DNA Loading on a Range of Gold Nanoparticle Sizes. *Anal. Chem.* **2006**, *78* (24), 8313–8318.
- (43) Reinhard, B. M.; Siu, M.; Agarwal, H.; Alivisatos, A. P.; Liphardt, J. Calibration of Dynamic Molecular Rulers Based on Plasmon Coupling between Gold Nanoparticles. *Nano Lett.* **2005**, *5* (11), 2246–2252.
- (44) Chakravorty, S.; Helb, D.; Burday, M.; Connell, N.; Alland, D. A Detailed Analysis of 16S Ribosomal RNA Gene Segments for the Diagnosis of Pathogenic Bacteria. *J. Microbiol Methods* **2007**, *69* (2), 330–339.